

## Photoinhibition of the quantum confined Stark effect in piezoelectric multiple quantum wells

J. L. Sánchez-Rojas, A. Sacedón, E. Calleja, and E. Muñoz

*Departamento Ingeniería Electrónica, Escuela Técnica Superior de Telecomunicación, Universidad Politécnica de Madrid, Ciudad Universitaria, 28040 Madrid, Spain*

A. Sanz-Hervás

*Departamento Tecnología Electrónica, Escuela Técnica Superior de Telecomunicación, Universidad Politécnica de Madrid, Ciudad Universitaria, 28040 Madrid, Spain*

G. De Benito and M. López

*Departamento Teoría de la Señal, Escuela Técnica Superior de Telecomunicación, Universidad Politécnica de Valladolid, Valladolid, Spain*

(Received 10 October 1995; revised manuscript received 13 February 1996)

We show that photoinduced space-charge buildup in piezoelectric [111]-oriented multiple quantum wells (MQW's), with average electric fields opposing the field in the barriers, inhibits the shifting of optical transitions by externally applied electric fields. This effect is due to the screening of the average electric field as photogenerated electrons and holes drift by this average field towards opposite locations in the MQW region. The resulting dipole flattens the envelope potential and hence precludes the change of energy levels with variations of external field. This behavior has been observed in different device configurations employing  $\text{In}_{1-x}\text{Ga}_x\text{As}/\text{GaAs}$  MQW embedded in a  $p$ - $i$ - $n$  diode by low-temperature photoluminescence (PL) and photocapacitance spectroscopies under different bias conditions. In addition to these "self-locked" transitions, we also observe other peaks in the PL spectra that result from the charge accumulation effect and that are qualitatively explained using Hartree calculations. [S0163-1829(96)01823-1]

Electric fields applied perpendicular to the layers of quantum heterostructures can drastically modify their energy levels<sup>1</sup> and absorption properties.<sup>2</sup> The quantum confined Stark effect (QCSE) is a large electroabsorption effect with device applications such as low-energy optical modulators and switches. In the usual symmetric quantum well (QW), this effect exhibits a quadratic dependence on the external electric field. A linear Stark effect can be obtained by means of different configurations such as asymmetric QW's with a variable composition,<sup>3</sup> coupled quantum wells,<sup>4</sup> and [111]-oriented strained multiple quantum wells (MQW's).<sup>5</sup> In the latter case, if strain-induced piezoelectric fields are large compared with the external fields, changes in the electronic structure and optical properties will vary linearly with the magnitude of the external field. Moreover, a blueshift in the optical transitions will be observed when the sign of the external voltage opposes that of the built-in field.<sup>6</sup> We have recently utilized this effect to obtain quantitative information about the piezoelectric constant of  $\text{In}_x\text{Ga}_{1-x}\text{As}$  for a range of In compositions.<sup>7</sup> In previous work, we have demonstrated that optical and electronic properties<sup>8</sup> are strongly dependent on the sign of the average electric field (AEF) in the MQW region. In this paper we show how, under certain design conditions (negative AEF), the optical transition energies in most of the QW's incorporated in the intrinsic region of a  $p$ - $i$ - $n$  diode are independent of external field. The essential requirements for this observation are shown to be the presence of a negative AEF together with a certain degree of coupling between QW's. We present the results obtained by photoluminescence (PL) in two different samples, and discuss observations using other spectroscopic tech-

niques. All of the samples studied show more than one peak (at least three) in the PL spectra under open circuit conditions. It is shown that the additional features are associated with a nonuniform field distribution in the structure, rather than impurity-related recombinations and that the assessment by PL of growth quality of unprocessed samples can be very difficult.

The samples analyzed in this work were grown by solid source molecular-beam epitaxy. The substrates were (111)B Si-doped GaAs misoriented  $1^\circ$  toward the [211] direction. Each device was composed of a  $p$ - $i$ - $n$  structure incorporating a  $0.57\text{-}\mu\text{m}$  intrinsic region between Si- and Be-doped  $n$ - (bottom) and  $p$ -type (top) layers. A MQW comprising N-strained  $\text{In}_x\text{Ga}_{1-x}\text{As}$  QW's was located at the center of the  $i$  region. Indium composition, well width ( $L_w$ ), and barrier width ( $L_b$ ) were specifically designed<sup>8</sup> and the real values of these three parameters were determined by high-resolution x-ray diffractometry (HRXRD). Sample *M10* had ten periods of  $86\text{-}\text{\AA}$   $\text{In}_x\text{Ga}_{1-x}\text{As}/130\text{-}\text{\AA}$  GaAs QW's and indium composition,  $x=0.17$ . Sample *M10W* had the same MQW structure as *M10*, but with QW Nos. 1 and 10 20% wider ( $L_w \sim 110\text{ \AA}$ ). Devices were isolated by wet chemical mesa etching. The top ( $p$ -type layer) contacts were annular rings of  $900\text{-}\mu\text{m}$  external diameter and  $400\text{-}\mu\text{m}$  internal diameter for optical access.

Because of the features present in the PL spectra, the assessment of sample quality by this technique was not possible. Instead, a HRXRD study was performed using a Bede  $D^3$  diffractometer in the low-resolution mode. We measured 111, 333, and  $224 \pm$  reflections at different azimuthal positions. The theoretical profiles were calculated with our own

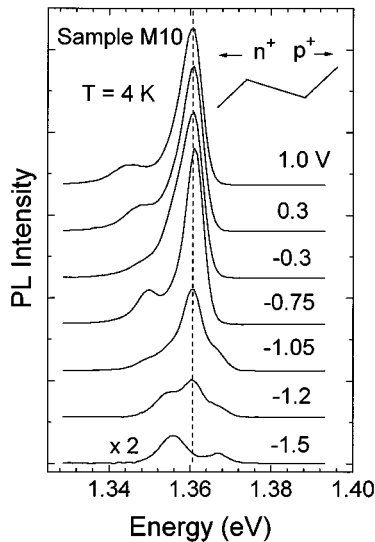


FIG. 1. Series of PL spectra for sample *M10* with the indicated bias voltage applied to the diode. The vertical dashed line is a guide to the eyes, showing the inhibition of the QCSE. The envelope of the potential profile for 0 V is sketched in the inset.

simulation program and fitted to the experimental scans by a trial and error procedure.<sup>9</sup> PL measurements were used to examine the effect of photogenerated carriers on the confined transition energies between bound states within the QW's. The samples were held in a cryostat at a temperature of 5 K although the evolution with temperature was also studied. Photoexcitation was provided by a cw Ti/sapphire laser pumped with an Ar-ion laser and tuned to 850 nm, so that barriers were not illuminated. The laser power was decreased until no significant changes in the PL spectra were observed ( $\sim 0.1$  mW).

Figure 1 shows the PL spectra measured in sample *M10* under selected bias voltages. The main peak, observed at  $\sim 1.36$  eV, remains at this energy over the whole range of voltages, for which it can be detected and before it is completely quenched. Electric-field-induced PL quenching<sup>10</sup> eventually occurs, due to the increasing rate of tunneling escape of electrons out of the QW's, relative to that of electron-hole recombination.

In addition to the high-intensity PL peak, the spectra taken under positive voltages exhibit a shoulder at lower energies. This small peak shows a blueshift with decreasing voltages (i.e., increasing electric fields opposing the piezoelectric fields). It appears again at  $\sim -0.5$  V, after merging the main peak, and shows a slight redshift. A third peak is observed at higher energies for voltages lower than  $\sim -1$  V. It should be noted that none of the PL peaks present in the spectra of Fig. 1 shows the behavior expected for impurity-related transitions, regarding evolution with laser power, temperature, or applied bias. Most importantly, the PL features and their evolution with voltage have been observed in all samples with the same or similar structure, where a single PL peak that blueshifts with decreasing voltage would be expected.<sup>8</sup> We attribute the multiple peak spectra to the charge accumulation resulting from an intrinsic negative average field in the MQW region (see inset in Fig. 1), causing photogenerated electrons (holes) to drift towards the  $p^+$  ( $n^+$ ) regions, so that they accumulate in the QW nearest to

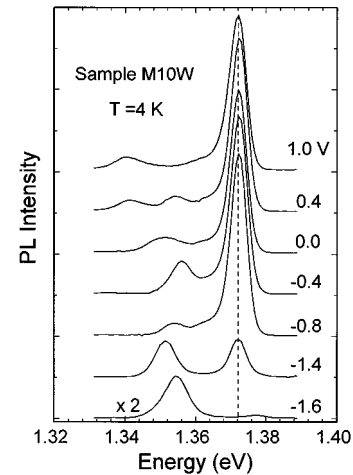


FIG. 2. Series of PL spectra for sample *M10W* with the indicated bias voltage applied to the diode. The vertical dashed line is a guide to the eyes, showing the inhibition of the QCSE. This effect occurs only in the transitions of the QW Nos. 2–9.

this region. The resulting dipole would have two main effects on the optical transitions: (i) screening of the external electric field within the MQW region, and (ii) shifting of the PL transition energies within the extreme QW's, where two-dimensional electron and hole gases are present. Since these extreme QW's are, therefore, expected to play a major role in the effects observed in Fig. 1, sample *M10W*, which has the same configuration as *M10*, but with wider QW Nos. 1 and 10 (110 Å), was designed to show these effects more clearly.

The behavior of the PL spectra of sample *M10W* (Fig. 2) is very similar to that of sample *M10*. The high-intensity peak has a spectral position independent of the applied bias, exhibiting a small blueshift just when its intensity becomes very low ( $\sim -1.6$  V). The peaks at lower energy correspond to the  $E_1$ -HH1 optical transitions in the wider QW's (Nos. 1 and 10). Despite the fact that both QW Nos. 1 and 10 have the same In composition and thickness, each gives a well-resolved PL peak under certain bias conditions. Furthermore, one of the peaks shows a clear “unexpected” redshift with decreasing bias followed by a strong blueshift (10 meV with a change of  $\sim 0.3$  V in the bias voltage).

The inhibition of the QCSE associated with charge accumulation in the MQW is not only detected by PL measurements. Another simple technique that we have recently used to characterize [111] MQW (Refs. 11 and 12) is photocapacitance spectroscopy.<sup>13</sup> In Fig. 3, we show the photocapacitance versus energy spectra measured in sample *M10* for different applied voltages and taken at a temperature  $T=4$  K. The illumination power was the same as for the spectra plotted in Fig. 1. Different excitonic transitions can be identified in the spectra of Fig. 3, corresponding to the  $E_i$ -HH $_j$  ( $i$ th electron level to  $j$ th heavy-hole level) energies as marked in the figure. The most remarkable observation is again the absence of a significant shift in the optical transitions in the range of negative average electric field (estimated to be from positive bias to  $\sim -0.5$  V). A clear blueshift is then observable for voltages lower than  $-1$  V, in agreement with our estimations. Note that the features present in the PL spectra of Fig. 1 are not resolved in the spectra of Fig. 3, although a voltage-dependent spectral

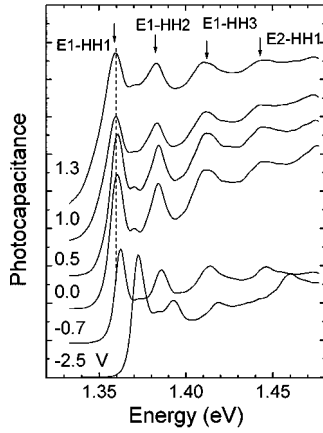


FIG. 3. Photocapacitance spectra for different bias voltages in sample *M10*. The origin of the excitonic peaks is marked for each transition. The vertical dashed line shows the inhibition of the QCSE.

broadening in the low-energy part of the excitonic peaks was observed.

In order to understand the anomalous behavior of the PL spectra, we have performed a self-consistent solution of the Schrödinger and Poisson equations, assuming a given amount of photogenerated electrons and holes in the structure. The QW's are considered to be in equilibrium with each other (constant quasi-Fermi levels throughout the MQW region) and the main limitation of our calculations is that many-body effects are neglected. However, the Schrödinger-Poisson calculations allows one to understand qualitatively two important effects systematically observed in the samples with negative average electric field, namely, the inhibition of the QCSE caused by a long-range screening effect and the splitting of the PL transition energies associated with the flat envelope potential conditions.

The effect of the photogenerated charge on the conduction-band (CB) potential profile of sample *M10* is shown in Fig. 4(a). Using the potential profile for a voltage of +1 V (dashed line) as the starting point of the self-consistent loop, the potential plotted with solid line in Fig. 4(a) results. The total sheet charge density (for both electrons and holes) was taken to be  $4 \times 10^{11} \text{ cm}^{-2}$ , the minimum concentration necessary to entirely screen the average electric field. The final self-consistent charge distribution  $\rho(z)$  [Fig. 4(a)] demonstrates the generation of a charge dipole with most of electrons (holes) accumulated in the QW nearest to the  $p^+$  ( $n^+$ ) region. We also observe a small contribution of in-well screening, i.e., small charge dipoles located at the intermediate QW's. This effect increases with increasing illumination power, and hence sheet charge density. Solving the self-consistent problem for different bias voltages, in the range of negative average fields (under dark conditions), does not change the resultant CB profile (solid line) significantly [the changes in the transition energies of the intermediate QW's (Nos. 2–9) are less than 2 meV]. This accounts for the inhibition of the QCSE for some optical transitions (Figs. 1–3) in the range of voltages for which the AEF is negative under dark conditions.

It can be seen in Fig. 4(a) that the field distribution is not uniform inside the MQW, in the sense that the average field

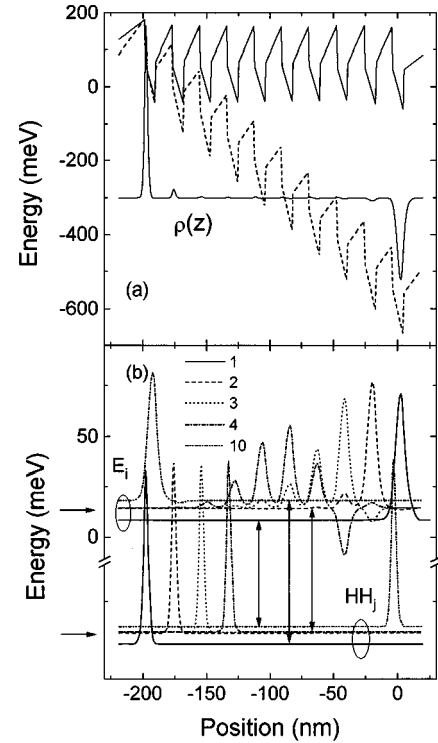


FIG. 4. (a) CB potential profiles under dark conditions and +1 V applied (dashed line) and with  $4 \times 10^{11} \text{ cm}^{-2}$  electrons and holes (solid line). The self-consistent distribution of charge is also shown. (b) Electron and hole wave functions for the levels 1, 2, 3, 4, and 10 (from low to high energy). The horizontal arrows mark the degenerated levels and the vertical arrows show the three possible transitions that explain the multiple peak PL spectra.

is approximately zero in the region of QW's Nos. 2–9, but there are changes in the potential of QW's Nos. 1 and 10 associated with the two-dimensional electron and hole gases forming the dopole. This effect leads us to interpret the splittings observed in the PL spectra (see Fig. 1) as originated from the energy-level splittings associated with the field inhomogeneities. This is clearly observed in Fig. 4(b), where we have plotted representative electron and hole wave functions of the first ten confined levels in the structure. The wave functions are superimposed on the energy value of the corresponding level (increasing electron and hole energies in the  $y$  axis).  $E$  (HH) levels are in the upper (lower) part of the figure. We observe that the eight ( $E$  or HH) levels corresponding to QW's Nos. 2–9 are almost degenerate [horizontal arrows in Fig. 4(b)]. However, there is a noticeable splitting of the energy levels  $i=1$  ( $j=1$ ) and  $i=10$  ( $j=10$ ), with respect to the rest of fundamental electron (hole) levels in QW Nos. 2–9. This fact gives rise to the three types of optical transitions sketched with vertical arrows in Fig. 4(b). They correspond to the  $E1$ -HH1 transition in (i) QW No. 1, (ii) QW No. 10, and (iii) the group of QW's Nos. 2–9. In our calculations, the magnitude of this splitting is always lower than the value observed experimentally. This discrepancy can be attributed to the presence of a considerable band-gap renormalization effect, due to the 2D electron and hole gases,<sup>14</sup> which is not included in the model.

In conclusion, we have shown an inhibition of the QCSE in  $\text{In}_x\text{Ga}_{1-x}\text{As}/\text{GaAs}$  MQW structures with different con-

figurations and the only requirements for these observations have been identified as a negative average electric field and a certain degree of coupling between QW's. In addition, a splitting of the energy levels associated with the extreme QW's, with respect to those of the rest of the QW's occurs. This splitting, which accounts for the observation of multiple PL peaks, is predicted by Hartree calculations for the structures. From the viewpoint of routine PL characterization of (111)B in  $\text{In}_x\text{Ga}_{1-x}\text{As}/\text{GaAs}$  MQW samples, the most important conclusion is that PL spectra do not give straightfor-

ward information about sample quality or structure parameters [as for (001) layers] when the average electric field is negative. In these samples, a full study by x-ray diffractometry is a more direct and accurate method.

The authors thank Dr. J. P. R. David (Sheffield University) for a discussion on the multiple PL peaks. This work was supported in part by the CICYT Project Nos. TIC95-0116, TIC93-0934, and TIC93-0912.

- 
- <sup>1</sup>E. E. Mendez, G. Bastard, L. L. Chang, L. Esaki, H. Morkoç, and R. Fischer, *Phys. Rev. B* **26**, 7101 (1982).
- <sup>2</sup>S. Schmitt-Rink, D. S. Chemla, and D. A. B. Miller, *Adv. Phys.* **38**, 2 (1989).
- <sup>3</sup>K. Nishi and T. Hiroshima, *Appl. Phys. Lett.* **51**, 320 (1987).
- <sup>4</sup>K. W. Steijn, R. P. Leavitt, and J. W. Little, *Appl. Phys. Lett.* **55**, 383 (1989).
- <sup>5</sup>C. Mailhiot and D. L. Smith, *Phys. Rev. B* **37**, 10 415 (1988).
- <sup>6</sup>E. A. Caridi, T. Y. Chang, K. W. Goossen, and L. F. Eastman, *Appl. Phys. Lett.* **56**, 659 (1990).
- <sup>7</sup>J. L. Sánchez-Rojas, A. Sacedón, F. González-Sanz, E. Calleja, and E. Muñoz, *Appl. Phys. Lett.* **65**, 2042 (1994).
- <sup>8</sup>J. L. Sánchez-Rojas, A. Sacedón, F. Calle, E. Calleja, and E. Muñoz, *Appl. Phys. Lett.* **65**, 2214 (1994).
- <sup>9</sup>A. Sanz-Hervás, A. Sacedón, E. J. Abril, J. L. Sánchez-Rojas, C. Villar, G. De Benito, M. Aguilar, M. Lopez, E. Calleja, and E. Muñoz (unpublished).
- <sup>10</sup>J. A. Kash, E. E. Mendez, and H. Morkoç, *Appl. Phys. Lett.* **46**, 173 (1985).
- <sup>11</sup>J. L. Sánchez-Rojas, A. Sacedón, E. Calleja, and E. Muñoz, *Appl. Phys. Lett.* **66**, 2223 (1995).
- <sup>12</sup>J. L. Sánchez-Rojas, A. Sacedón, A. Sanz-Hervás, E. Calleja, E. Muñoz, E. J. Abril, M. Aguilar, and M. López, *Semicond. Sci. Technol.* **10**, 1173 (1995).
- <sup>13</sup>R. Rosencher, N. Vodjdani, J. Nagle, P. Bois, E. Costard, and S. Delaitre, *Appl. Phys. Lett.* **55**, 1853 (1989).
- <sup>14</sup>P. Boring, B. Gil, and K. J. Moore, *Phys. Rev. Lett.* **71**, 1875 (1993).